Inorganic Chemistry

Article

pubs.acs.org/IC

Ligand Exchange and Redox Processes in Iridium Triazolylidene Complexes Relevant to Catalytic Water Oxidation

Ana Petronilho,[†] Antoni Llobet,*[,‡] and Martin Albrecht*[,†]

[†]School of Chemistry and Chemical Biology, University College Dublin, Belfield, Dublin 4, Ireland

[‡]Institute of Chemical Research of Catalonia (ICIQ), Av. Països Catalans 16, 43007 Tarragona, Spain

Supporting Information

ABSTRACT: Iridium(III) complexes containing a bidentate spectator ligand have emerged as powerful catalyst precursors for water oxidation. Here we investigate the initial steps of the transformation at the iridium center when using complex [IrCp*(pyr-trz)Cl] **1** (Cp* = pentamethylcyclopentadienyl, pyr-trz = 4-(2-pyridyl)-1,2,3-triazol-5-ylidene), a potent water oxidation catalyst precursor. Ligand exchange with water is facile and is reversed in the presence of chloride ions, while MeCN substitution is effective only from the corresponding aqua complex. A pK_a of 8.3 for the aqua complex was determined, which is in agreement with strong electron donation from the triazolylidene ligand that is comparable to aryl anions. Evaluation of the pH-dependent oxidation process in aqueous media reveals two regimes (pH 4−8.5 and above pH 10.5) where proton-coupled electron transfer processes occur. These investigations will help to further optimize water oxidation catalysts and indicate that MeCN as a cosolvent has adverse effects for initiating water coordination in the oxidation process.

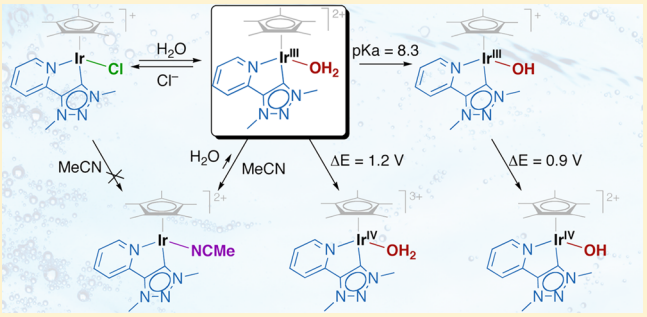

INTRODUCTION

Artificial photosynthesis through solar water splitting is one of the key technologies currently considered for harvesting and storing transient solar energy.[1−4] A major hurdle in this endeavor is the highly demanding water oxidation half-cycle, which requires the shuttling of four protons and four electrons to generate O_2.[5] Over the past few years, iridium complexes have emerged as very powerful catalysts for this water oxidation process.[6−18] Depending on the ligand design, very high turnover numbers have been achieved.[19]

Moreover, kinetic and mechanistic studies have provided increasingly compelling evidence that some complexes are precursors for homogeneous rather than heterogeneous[20−22] water oxidation catalysts and that the oxidation therefore occurs at an iridium center that is in a well-defined environment.[19,23−28] This environment has remained elusive to date despite various efforts to trap and isolate catalytically competent species.[29−32] In particular, iridium cyclopentadienyl complexes $[Ir(Cp^*)(L,L)X]^+$ ($Cp^* = C_5Me_5^-$) containing a chelating N,N-, C,N-, or C,C-bidentate ligand motif afforded high catalytic activity.[7−9,17,19,33,34] Postreaction analyses strongly indicate oxidative degradation of the Cp* ligand[27,32,33] rather than formation of IrO_x nanoparticles as a heterogeneous catalyst phase. These reactivity patterns underline the relevance of the initial steps of the transformation at the iridium center as a concept to understand and improve the catalytic activity and to reduce the catalyst activation barrier. To this end, we have investigated in more detail complex **1** as a representative for the recently discovered highly active water oxidation catalysts comprising a carbenic spectator ligand bound to an Ir(Cp*) unit (Figure 1).[3] Complex **1** is highly active in cerium(IV)-mediated water oxidation and achieves turnover numbers in excess of 40 000, thus providing a valuable system for detailing initial ligand substitution and redox processes. In addition, previous work on this complex, including detailed kinetic analyses as well as in situ monitoring of water oxidation by dynamic light scattering and NMR spectroscopy demonstrated that the catalytically active species is well-defined and thus homogeneous rather than a less reproducible heterogeneous layer.[19] The studies reported here detail ligand exchange as well as proton and electron donor/acceptor behavior of complex **1** and thus shed light on the accessibility of proton-coupled electron transfer (PCET) processes. These results highlight the relevance of the reaction conditions, in particular with respect to added cosolvents.

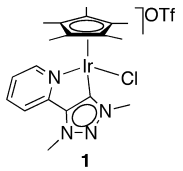

1

Figure 1. Water oxidation precatalyst iridium complex **1** containing an N,C-bidentate pyridyl−triazolylidene ligand.

Received: August 5, 2014
Published: November 21, 2014

RESULTS AND DISCUSSION

Ligand Exchange Propensity. Complexes **1**–**3** were synthesized as the triflate salts according to established procedures (Scheme 1).[19] Their behavior in solution was studied in detail. In D_2O, the chloro complex **1** coexists in a concentration-dependent equilibrium with the dicationic solvento complex **2**, as indicated by the appearance of two sets of pyridine resonances in the ^{1}H NMR spectrum. The equilibrium is shifted toward **1** in the presence of chloride ions (HCl, NR_4Cl), while the addition of HNO_3 (1 M) shifts the equilibrium toward the solvento complex **2**. Likewise, **2** is dominant in a 0.1 M aqueous NaOAc solution and becomes the exclusive species if the NaOAc concentration is raised to 1 M. These results indicate that solvolysis of **1** is promoted by ionic strength in addition to pH modifications (acid strength). Hydrolysis has also been observed in related anticarcinogenic $[Ir(Cp^*)Cl(L,L)]^+$ complexes under physiological conditions (e.g., L,L = 2,2′-bipyridine (bpy)).[35,36]

Scheme 1. Equilibria of Complexes 1, 2, and 3 in Different Solvents

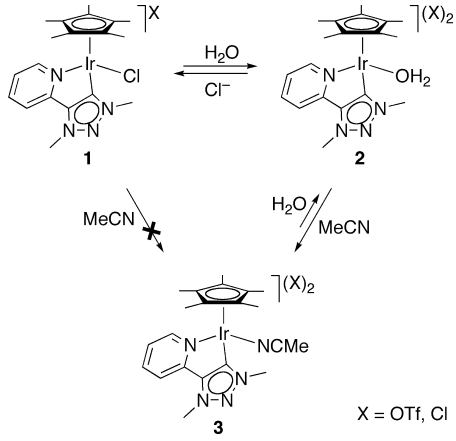

In contrast to this behavior in water, no chloride dissociation was detected when complex **1** was dissolved in MeCN. Strong chloro coordination to iridium is indicated by the chemical shift of the pyridyl protons at the β and γ positions at δ_H = 8.07 and 8.15 ppm, respectively (cf. δ_H = 8.14 and 8.27 ppm for the corresponding solvento complex **3**). The robustness of the Ir–Cl bond of **1** in MeCN is in agreement with the lower polarity of MeCN versus H_2O and reflects the low solvation of Cl^- in MeCN compared with water. These differences suggest a negative impact of MeCN as a (co)solvent for catalytic applications because the reduced ionic strength imparted by MeCN does not favor substitution of the chloro ligand.

To probe the coordination strength of MeCN and H_2O to the $[Ir(Cp^*)(C_{trz}\text{^}N_{py})]^{2+}$ unit ($C_{trz}\text{^}N_{py}$ = 1,3-dimethyl-4-(2-pyridyl)triazol-5-ylidene), the dicationic aqua complex **2** was dissolved in MeCN, and the other way around, the corresponding MeCN complex **3** was dissolved in D_2O. The ^{1}H NMR spectrum of **2** in CD_3CN features only one set of signals with chemical shifts identical to those of **3** in MeCN, thus indicating complete displacement of the D_2O ligand in **2** by MeCN. Conversely, a solution of the MeCN complex **3** in D_2O reveals two sets of signals due to a mixture of complexes **2** and **3** (in a 2:3 ratio). The two complexes are distinguished most diagnostically by the low-field doublets of the pyridyl α proton at δ_H = 9.10 and 9.01 ppm for **2** and **3**, respectively. The remaining pyridyl protons are magnetically identical in both complexes. Additionally, integration of the resonances for free and coordinated MeCN at 2.38 and 2.06 ppm corroborates the 2:3 ratio of **2** and **3**. These results reveal that the substitution of MeCN in **3** with water is highly unfavored and is only partial even in pure water under NMR conditions. Notably, when an aqueous solution of the MeCN complex **3** is diluted from 10 to 1.6 mM, the equilibrium is shifted from the initial 2:3 ratio completely toward **2** (Figure S1 in the Supporting Information).[37]

Thus, under catalytically relevant conditions (low iridium loading), the aqua complex is the prevailing species when starting from the chloro complex **1** or the MeCN complex **3**. However, when MeCN is used as a (co)solvent, iridium(III) has a strong preference to bind to this ligand rather than to water, and complex **3** becomes the dominant species, with obvious implications for analysis and (catalytic) activity.

Determination of pK_a. The pK_a of complex **2** was determined by spectroscopic titration using aqueous solutions buffered at different pH values.[38,39] Representative UV–vis spectra of the acidic and basic forms are depicted in Figure 2.

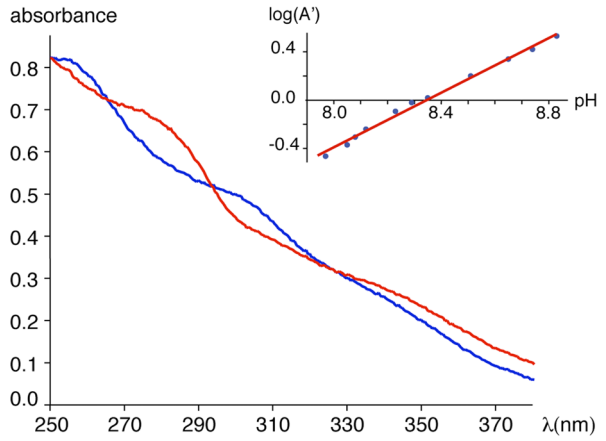

Figure 2. Representative UV spectra of complex **2** (0.06 mM in phosphate buffer at 0.1 M ionic strength) at pH 6.3 (blue line) and pH 11.0 (red line). The inset shows the correlation between pH and the logarithm of the absorbance at λ = 305 nm for complex **2**, with $\log(A') = \log[(A - A_{acid})/(A_{basic} - A)]$.

The yellow color of the complex solution was persistent, and modification of the pH did not result in a visual change in the absorption characteristics. While measurements were run over the entire UV–vis range (200–800 nm), spectroscopic changes pertained only to the UV region of the spectrum (200–400 nm), where complex **2** and its conjugate base showed distinctly different behaviors. At pH 6, maxima were observed at 255 and 305 nm (ε = 1600 and 1000 L mol^{-1} cm^{-1}, respectively) with a shoulder at around 350 nm, while at pH 11, two maximum were located at 280 and 340 nm (ε = 1400 and 600 L mol^{-1} cm^{-1}, respectively). Results from monitoring of the pH dependence of the absorbance at 305 nm are shown in the inset of Figure 2 (also see Figures S2 and S3).

Deduction of the pK_a value from the changes in absorption at 305 and 280 nm was hampered by the relatively small changes in extinction coefficient, hence providing data with limited accuracy (pK_a = 7.9 ± 0.2). Analysis based on the Henderson–Hasselbach equation, i.e., by correlating the logarithm of the absorbance versus pH at the wavelengths with diagnostic changes (Figure 2 inset), gave a slightly higher pK_a. The data

dx.doi.org/10.1021/ic501894u | Inorg. Chem. 2014, 53, 12896–12901

points at λ = 305 nm afforded pK_a = 8.35, whereas evaluation of the data points at λ = 280 nm provided pK_a = 8.25. Averaging these values suggests a pK_a value of 8.3 ± 0.1 for complex **2** (also see the Pourbaix diagram in Figure 5).

Previous studies indicated that monoaqua complexes $[IrCp^*(L,L)(H_2O)]^{2+}$ (L = N or O donor ligand) are less acidic than the corresponding trisaqua complex $[IrCp^*(H_2O)_3]^{2+}$.[40] The pK_a values have also been used to extrapolate the donor ability of the bidentate (L,L) ligand,[35,36] with a higher pK_a value corresponding to an increased donor capacity of the chelating ligand. The pK_a value obtained for complex **2** supports stronger donation by the neutral C,N-bidentate-chelating triazolylidene ligand compared with neutral N,O- or N,N-bidentate chelates (e.g., pK_a ≈ 7.2 ± 0.3 for L,L = bpy). It is slightly lower than the pK_a of the complex $[IrCp^*(ppy)(H_2O)]^{2+}$ containing the anionic and therefore supposedly stronger-donating 2-phenylpyridine (ppy) ligand (pK_a = 8.75).[35] These values underpin the unique ligand characteristics of mesoionic carbenes as donors intermediate between classically neutral and anionic ligands. We also note that the obtained pK_a value is in excellent agreement with the pK_a deduced from the Pourbaix diagram (see Figure 5). A similarly strong influence of the carbene ligand on the electronic properties was also noted for related ruthenium complexes.[41]

Obviously, the direct correlation of pK_a with donor properties requires caution if the ligand features proton donor/acceptor groups. In such complexes, the pK_a cannot be related exclusively to the donor capacity of the ligand and may be dominated by cooperative hydrogen transfer from coordinated water to such ligands.[22,34,42] In 1,2,3-triazolylidene complexes, the lone pair at the triazole N2 site[43−45] as well as the mesoionic character of the carbene[46] may potentially be involved in cooperative hydrogen transfer.

Electrochemical Analysis. The electrochemical behavior of complexes **1** and **2** was studied by cyclic voltammetry (CV) and differential pulse voltammetry (DPV) in water, CH_2Cl_2, and MeCN. For complex **2**, the measurements were also performed at various pHs, and a Pourbaix diagram was constructed from the potentials obtained by DPV measurements. No deposition or decomposition of the complexes was detected in any of the measurements, nor did an increase in the electrocatalytic water oxidation current occur upon successive scans, which would hint toward the formation of iridium oxide.[21]

In H_2O, complexes **1** and **2** display essentially identical electrochemical behavior, in agreement with the ligand exchange processes described above. A major oxidation wave at +1.21 V vs SCE is observed at pH 1 (Figure 3), indicating that chloride oxidation does not interfere with the first oxidation at iridium in **1**. The measurements further underline that in aqueous acidic solution (e.g., aqueous ceric ammonium nitrate) it is irrelevant whether the chloro complex **1** or its aqua analogue **2** is used as the catalyst precursor for water oxidation and that both complexes generate the same oxidized species at low pH. The observed oxidation potential is almost 300 mV lower than that reported for analogous complexes with bpy-derived ligands,[35] corroborating the stronger donor properties of the triazolylidene compared with pyridine. Complexes **1** and **2** reveal very similar behavior at higher pH values also (Figure S3). At pH 7, two oxidation curves were identified by DPV. The second oxidation wave is more intense for compound **1**, which may speculatively be due to an overlap with the oxidation of the fraction of complex **1** that has not undergone solvolysis.

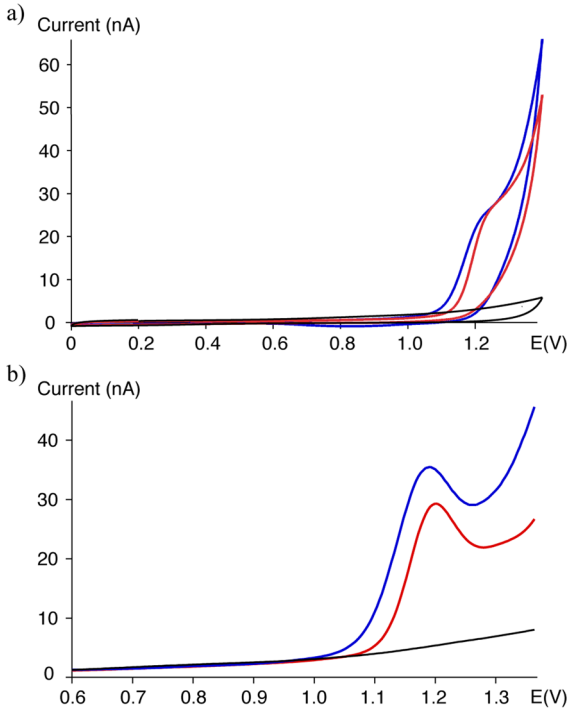

Figure 3. Representative (a) cyclic voltammograms and (b) differential pulse voltammograms for complexes **1** (1.3 mM, blue line) and **2** (1.1 mM, red line) at pH 1.1 (0.1 M HNO_3) at a scan rate of 30 mV s^{-1}. The background currents are shown in black. *E* values are in V vs SCE.

At pH 11, where complex **2** is almost fully deprotonated and contains the hydroxo ligand (hydroxo/aqua ratio = 500:1; cf. the pK_a determination above), one major oxidation wave is detected for both complexes at lower potential (+0.84 V vs SCE). This lower oxidation potential is in agreement with the stronger donor properties of OH^- compared with neutral H_2O.

Because of potential complications imparted by the Cl^-/H_2O ligand exchange equilibrium with complex **1** upon pH modification, all further analyses were performed with the aqua complex **2** (X = OTf). This complex was investigated between pH 0 and pH 12.5 at 0.5 pH unit increments to fully map its electrochemical behavior. The CV and DPV experiments were mutually consistent, and hence, pertinent potentials were extracted from the latter. Representative DPV traces at selected pH values (Figure 4) reveal two different oxidation processes,[47] though the second process is often shallow and not well-resolved (cf. the trace at pH 9.1). This second oxidation wave was detected only in the DPV measurements, suggesting a fast process that is tentatively attributed to a second iridium oxidation. Catalytic solvent oxidation was induced upon further increases in the potential in all of the measurements.

When considering the pH dependence of the first oxidation process, four specific regions can be distinguished (Figure 5): below pH 4 and in the pH range 8.5−10.5, the oxidation process is pH-independent, whereas a pH-dependent oxidation potential is observed in the pH ranges 5.5−8.5 and 10.5−12.5. Accordingly, the constant oxidation potential at low pH suggests an electron transfer that does not involve proton shuttling, i.e., oxidation of $Ir^{III}-OH_2$ (**2**) to an $Ir^{IV}-OH_2$ species ($\mathbf{2}^+$). Above pH 4, a pH-dependent electron transfer occurs. The slope of the pH dependence is linear with a slope of 61 ± 5 mV/pH unit (Figure S4), which is very close to the

dx.doi.org/10.1021/ic501894u | *Inorg. Chem.* 2014, 53, 12896−12901

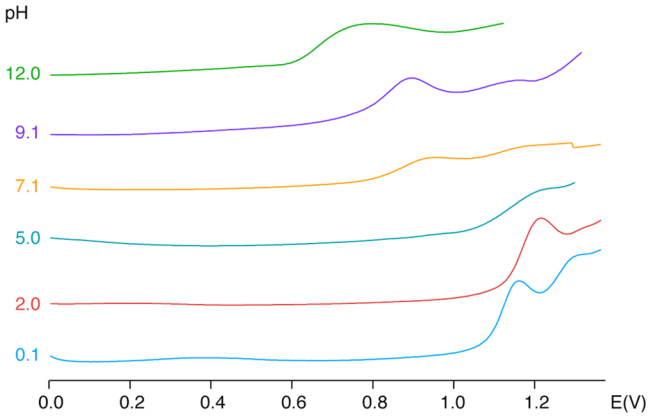

Figure 4. Differential pulse voltammetry of compound **2** in water at various pHs. *E* values are in V vs SCE. All of the solutions were pH-buffered and at 0.1 M ionic strength (see the SI for buffer preparation details).

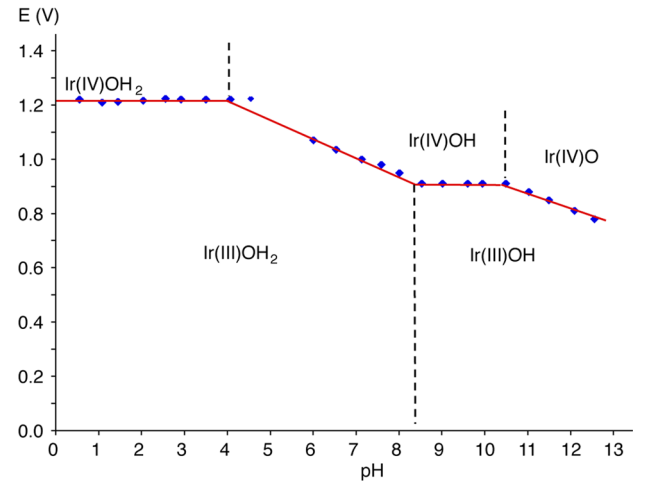

Figure 5. Pourbaix diagram for complex **2** in water (oxidation potentials *E* from DPV in V vs SCE).

theoretically predicted slope of 59 mV/pH unit for a $1H^+/1e^-$ process according to the Nernst law.[48] Hence, a PCET process is indicated in this regime, involving a net transformation of $Ir^{III}-OH_2$ complex **2** to an $Ir^{IV}-OH$ complex. Further increasing the pH leads again to a pure electron transfer ($Ir^{III}-OH$ to $Ir^{IV}-OH$ in the pH 8.5–10.5 region). At higher pH (pH above 10.5), another $1H^+/1e^-$ process is revealed by the linear correlation between the oxidation potential and the pH (slope = 63 ± 5 mV/pH unit; Figure S5), starting from deprotonated $Ir^{III}-OH$ to produce $Ir^{IV}=O$ by PCET. Such a model is in agreement with an increasing relevance of the hydroxide species as the pK_a value is approached.

The redox potential of the naturally occurring oxygen-evolving complex in photosystem II is known to be leveled through PCET processes,[49,50] which enable consecutive redox processes without the buildup of charge. This effect has been noted with synthetic catalysts based on ruthenium as well[51] and may rationalize the observation of only one oxidation process under basic conditions. The pH dependence of the oxidation potential of complex **2** and specifically the lower onset potential under basic conditions further support the occurrence of PCET also in complex **2**, which may play a critical role in providing a energetically viable catalytic cycle and in enabling high turnover numbers.

Electrochemical measurements on the iridium complex **2** in MeCN disclose significantly different behavior. While the substitution of H_2O as a ligand with MeCN is fast and essentially complete upon dissolution, the monocationic chloro complex **1** is inert toward a similar exchange, with the chloro ligand remaining coordinated. This difference in reactivity for the two complexes **1** and **2** in MeCN is also reflected in their electrochemical properties. Complex **2** (in fact complex **3**) undergoes an irreversible oxidation at high potential (+1.48 V vs SCE; Figure 6). In contrast, oxidation of complex **1** occurs

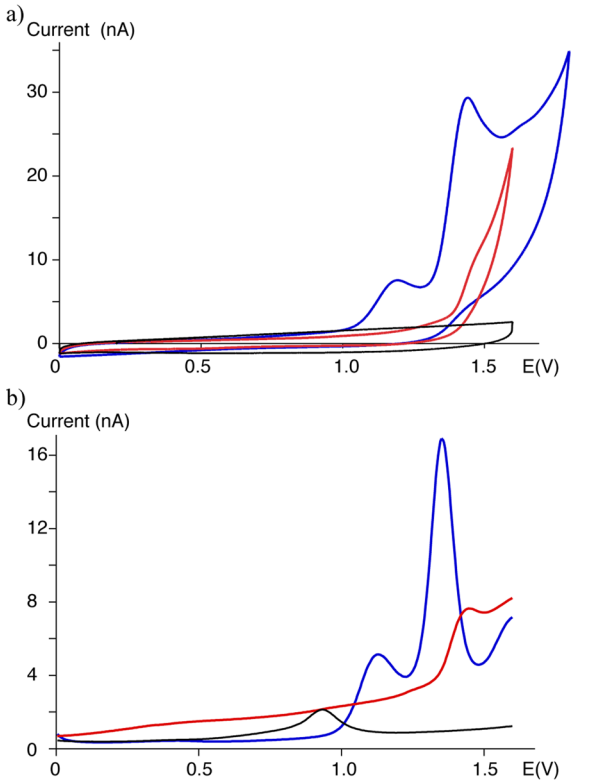

Figure 6. Representative plots from (a) cyclic voltammetry and (b) differential pulse voltammetry for complexes **1** (1.4 mM, blue curve) and **2** (1.2 mM, red curve) in MeCN containing 0.1 M $Bu_4N(PF_6)$ as a supporting electrolyte at a scan rate of 30 mV s^{-1} scan rate. The background currents are shown in black. *E*values are in V vs SCE.

already at E_1 = +1.13 V vs SCE. The lower oxidation potential of complex **1** is in agreement with the stronger donor ability of anionic Cl^- compared with the neutral MeCN ligand in **3** and also reflects the slight π-acceptor character of MeCN. DPV of complex **1** showed a second oxidation at E_2 = +1.36 V vs SCE. A related two-step oxidation has been described for similar iridium chloro complexes[17,29] and has been attributed to the intermediate formation of an unstable Ir(IV)–Cl species that decomposes to give Ir(III) and Cl_2 gas.[29] While the first oxidation potential is similar for complex **1** and related complexes (around +1.1 V vs SCE), the second potential observed with complex **1** is significantly lower (+1.36 vs +1.6 V vs SCE) and may thus be associated either with the specific properties of the triazolylidene ligand or, more likely, with electrocatalytic oxidation of residual water in the MeCN solvent. Support for the latter is provided by the catalytic nature of the measured current. When measured in CH_2Cl_2,

dx.doi.org/10.1021/ic501894u | *Inorg. Chem.* 2014, 53, 12896–12901

complexes **1** and **2** display almost identical oxidation potentials (+1.47 and +1.48 V vs SCE; Figure S6), indicating that in nonaqueous solutions, PCET from the aqua complex occurs at about the same potential as the oxidation of the chloro complex.[52] This similarity is obviously a consequence of the tight binding of the H_2O ligand in CH_2Cl_2 but not in MeCN.

This work aligns well with previous studies of the pH-dependent oxidation potentials of related iridium(III) complexes. For example, an analogue of complex **1** featuring bpy rather than the pyridyl−carbene as the L,L-type ligand was evaluated in the pH 7−12 range and revealed a first oxidation potential that could be distinguished from the catalytic solvent oxidation only at high pH.[10] At pH <7, no oxidation was detected with the bpy analogue, which demonstrates the stronger donor ability of the triazolylidene ligand in **1** compared with the pyridine in the bpy analogue. This easier accommodation of high-valent intermediates may be a key factor for the high catalytic robustness and high turnover numbers accomplished by complex **1**. The pH dependence of a carbene-containing iridium(III) complex has also been reported very recently; the complex $[Ir(Cp^*)(NHC)(OH)]^+$ is formally a pentacoordinate iridium complex (NHC = *N*,*N*′-dimethylimidazol-2-ylidene) that forms a dimer with a bis(μ-oxo) diiridium core.[53] Such a process is presumably prevented in **1** because of the rigid chelation of the pyridyl−triazolylidene ligand. Finally, a pH-dependent investigation has also been reported for an iridium(III) bpy complex that was attached to the surface of an indium tin oxide electrode via a phosphonate or carboxyl end group bound to the bpy ligand.[54] Under these conditions, the pH-dependent redox behavior is substantially different from that of **1**, probably because of the restricted translational mobility and also because the nature of the second coordination sphere can be radically different in anchored systems. In addition, these anchored complexes lose the molecular homogeneous signature of the precursor complexes, which might suggest the formation of a heterogeneous phase containing IrO_x species. Such simple oxides anchored onto surfaces follow Nernstian behavior when analyzed at different pH,[55] in sharp contrast to complex **1** (cf. Figure 5).

CONCLUSIONS

In water, the iridium chloro complex transforms essentially quantitatively to the aqua complex **2** via rapid chloride dissociation, indicating that in aqueous media the (catalytically) active species is identical irrespective of whether **1** or **2** is used as the precursor. Accordingly, the electrochemical behavior in water is identical irrespective of the starting complex used. The oxidation potential of complex **2** is pH-independent under acidic conditions yet strongly pH-dependent in neutral and basic media. The slope of the plot of potential versus pH indicates the accessibility of $1H^+/1e^-$ processes, in line with a proton-coupled electron transfer (PCET) process. While the measured oxidation represents only a first step en route to water oxidation, these insights may provide further guidelines for detailing the catalyst activity, especially when using less acidic conditions than those imparted by cerium(IV)-mediated water oxidation.

Significantly, complex **1** displays behavior distinctly different from that of **2** in MeCN. These observations emphasize the relevance of the conditions used and indicate that different species can be involved if coordinating solvents other than water are used in water oxidation catalysis, e.g., as additives. The use of MeCN therefore substantially increases the complexity of the catalytic system, and the relevant active species become even less evident. Our results indicate that specifically oxidation processes are markedly affected when using such coordinated solvents.

EXPERIMENTAL SECTION

The syntheses of complexes **1**−**3** were described previously.[19] All of the electrochemical experiments were performed with a Biologic SP-150 potentiostat using a three-electrode cell composed of a glassy carbon disk (3 mm diameter, CH instruments) as the working electrode, a platinum disk (2 mm diameter) from CH Instruments as an auxiliary electrode, and a saturated calomel electrode (BAS Japan) as the reference electrode. The experiments in MeCN and CH_2Cl_2 contained NBu_4PF_6 (0.1 M) as a supporting electrolyte. Measurements in aqueous solutions were performed at different pH as follows: For pH 0−1.5, aqueous HNO_3 solutions (0.1 M) were titrated with NaOH (1 M) to the desired pH; for pH >1.5, aqueous solutions were prepared using different phosphate, acetate, or carbonate buffers at 0.1 M ionic strength, and their detailed preparation is included in the Supporting Information. UV measurements were performed with an Agilent Cary 50 UV−vis spectrophotometer.

ASSOCIATED CONTENT

Supporting Information

Representative NMR spectra, spectroscopic pK_a determination data, and details related to electrochemical measurements and aqueous buffer preparation. This material is available free of charge via the Internet at http://pubs.acs.org.

AUTHOR INFORMATION

Corresponding Authors

*E-mail: martin.albrecht@ucd.ie.

*E-mail: allobet@iciq.cat.

Notes

The authors declare no competing financial interest.

ACKNOWLEDGMENTS

We thank Ariana Savini and Carlo Di Giovanni for technical assistance and Johnson Matthey for a generous loan of iridium. This work was supported financially by Science Foundation Ireland (SRC), the European Research Council (PoC-324609, CoG-615653), and MINECO (Grant CTQ-2013-49075-R).

REFERENCES

(1) Bard, A. J.; Fox, M. A. *Acc. Chem. Res.* **1995**, *28*, 141−145.
(2) Hammarström, L.; Hammes-Schiffer, S. *Acc. Chem. Res.* **2009**, *42*, 1859−1860 (thematic issue).
(3) McDaniel, N. D.; Bernhard, S. *Dalton Trans.* **2010**, *39*, 10021−10030.
(4) Reece, S. Y.; Hamel, J. A.; Sung, K.; Jarvi, T. D.; Esswein, A. J.; Pijpers, J. J. H.; Nocera, D. G. *Science* **2011**, *334*, 645−648.
(5) *Molecular Water Oxidation Catalysis*; Llobet, A., Ed..; Wiley: Chichester, U.K., 2014.
(6) McDaniel, N. D.; Coughlin, F. J.; Tinker, L. L.; Bernhard, S. *J. Am. Chem. Soc.* **2008**, *130*, 210−217.
(7) Hull, J. F.; Balcells, D.; Blakemore, J. D.; Incarvito, C. D.; Eisenstein, O.; Brudvig, G. W.; Crabtree, R. H. *J. Am. Chem. Soc.* **2009**, *131*, 8730−8731.
(8) Lalrempuia, R.; McDaniel, N. D.; Müller-Bunz, H.; Bernhard, S.; Albrecht, M. *Angew. Chem., Int. Ed.* **2010**, *49*, 9765−9768.
(9) Savini, A.; Bellachioma, G.; Ciancaleoni, G.; Zuccaccia, C.; Zuccaccia, D.; Macchioni, A. *Chem. Commun.* **2010**, *46*, 9218−9219.
(10) Blakemore, J. D.; Schley, N. D.; Balcells, D.; Hull, J. F.; Olack, G. W.; Incarvito, C. D.; Eisenstein, O.; Brudvig, G. W.; Crabtree, R. H. *J. Am. Chem. Soc.* **2010**, *132*, 16017−16029.

(11) Dzik, W. I.; Calvo, S. E.; Reek, J. N. H.; Lutz, M.; Ciriano, M. A.; Tejel, C.; Hetterscheid, D. G. H.; de Bruin, B. *Organometallics* **2011**, *30*, 372−374.
(12) Parent, A. R.; Blakemore, J. D.; Brudvig, G. W.; Crabtree, R. H. *Chem. Commun.* **2011**, *47*, 11745−11747.
(13) Moore, G. F.; Blakemore, J. D.; Milot, R. L.; Hull, J. F.; Song, H. Y.; Cai, L.; Schmuttenmaer, C. A.; Crabtree, R. H.; Brudvig, G. W. *Energy Environ. Sci.* **2011**, *4*, 2389−2392.
(14) Parent, A. R.; Brewster, T. P.; De Wolf, W.; Crabtree, R. H.; Brudvig, G. W. *Inorg. Chem.* **2012**, *51*, 6147−6152.
(15) Petronilho, A.; Rahman, M.; Woods, J. A.; Al-Sayyed, H.; Müller-Bunz, H.; MacElroy, D. J.; Bernhard, S.; Albrecht, M. *Dalton Trans.* **2012**, *41*, 13074−13080.
(16) Savini, A.; Bellachioma, G.; Bolaño, S.; Rocchigiani, L.; Zuccaccia, C.; Zuccaccia, D.; Macchioni, A. *ChemSusChem* **2012**, *5*, 1415−1419.
(17) Bucci, A.; Savini, A.; Rocchigiani, L.; Zuccaccia, C.; Rizzato, S.; Albinati, A.; Llobet, A.; Macchioni, A. *Organometallics* **2012**, *31*, 8071−8074.
(18) Codola, Z.; Cardoso, J. M. S.; Royo, B.; Costas, M.; Lloret-Fillol, J. *Chem.—Eur. J.* **2013**, *19*, 7203−7213.
(19) Woods, J. A.; Lalrempuia, R.; Petronilho, A.; McDaniel, N. D.; Müller-Bunz, H.; Albrecht, M.; Bernhard, S. *Energy Environ. Sci.* **2014**, *7*, 2316−2328.
(20) Grotjahn, D. B.; Brown, D. B.; Martin, J. K.; Marelius, D. C.; Abadjian, M.-C.; Tran, H. N.; Kalyuzhny, G.; Vecchio, K. S.; Specht, Z. G.; Cortes-Llamas, S. A.; Miranda-Soto, V.; van Niekerk, C.; Moore, C. E.; Rheingold, A. L. *J. Am. Chem. Soc.* **2011**, *133*, 19024−19027.
(21) Hetterscheid, D. G. H.; Reek, J. N. H. *Chem. Commun.* **2011**, *47*, 2712−2714.
(22) Hong, D.; Murakami, M.; Yamada, Y.; Fukuzumi, S. *Energy Environ. Sci.* **2012**, *5*, 5708−5716.
(23) Schley, N. D.; Blakemore, J. D.; Subbaiyan, N. K.; Incarvito, C. D.; D'Souza, F.; Crabtree, R. H.; Brudvig, G. W. *J. Am. Chem. Soc.* **2011**, *133*, 10473−10481.
(24) Junge, H.; Marquet, N.; Kammer, A.; Denurra, S.; Bauer, M.; Wohlrab, S.; Gärtner, F.; Pohl, M.-M.; Spannenberg, A.; Gladiali, S.; Beller, M. *Chem.—Eur. J.* **2012**, *18*, 12749−12758.
(25) Wang, C.; Wang, J.-L.; Lin, W. *J. Am. Chem. Soc.* **2012**, *134*, 19895−19908.
(26) deKrafft, K. E.; Wang, C.; Xie, Z.; Su, X.; Hinds, B. J.; Lin, W. *ACS Appl. Mater. Interfaces* **2012**, *4*, 608−613.
(27) Hintermair, U.; Hashmi, S. M.; Elimelech, M.; Crabtree, R. H. *J. Am. Chem. Soc.* **2012**, *134*, 9785−9795.
(28) Petronilho, A.; Woods, J. A.; Bernhard, S.; Albrecht, M. *Eur. J. Inorg. Chem.* **2014**, 708−714.
(29) Brewster, T. P.; Blakemore, J. D.; Schley, N. D.; Incarvito, C. D.; Hazari, N.; Brudvig, G. W.; Crabtree, R. H. *Organometallics* **2011**, *30*, 965−973.
(30) Zuccaccia, C.; Bellachioma, G.; Bolaño, S.; Rocchigiani, L.; Savini, A.; Macchioni, A. *Eur. J. Inorg. Chem.* **2012**, 1462−1468.
(31) Savini, A.; Belanzoni, P.; Bellachioma, G.; Zuccaccia, C.; Zuccaccia, D.; Macchioni, A. *Green Chem.* **2011**, *13*, 3360−3374.
(32) Savini, A.; Bucci, A.; Bellachioma, G.; Rocchigiani, L.; Zuccaccia, C.; Llobet, A.; Macchioni, A. *Chem.—Eur. J.* **2014**, *20*, 690−697.
(33) Wang, C.; Xie, Z.; Dekrafft, K. E.; Lin, W. *J. Am. Chem. Soc.* **2011**, *133*, 13445−13454.
(34) DePasquale, J.; Nieto, I.; Reuther, L. E.; Herbst-Gervasoni, C. J.; Paul, J. J.; Mochalin, V.; Zeller, M.; Thomas, C. M.; Addison, A. W.; Papish, E. T. *Inorg. Chem.* **2013**, *52*, 9175−9183.
(35) Liu, Z.; Habtemariam, A.; Pizarro, A. M.; Fletcher, S. A.; Kisova, A.; Vrana, O.; Salassa, L.; Bruijnincx, P. C. A.; Clarkson, G. J.; Brabec, V.; Sadler, P. J. *J. Med. Chem.* **2011**, *54*, 3011−3026.
(36) Liu, Z.; Habtemariam, A.; Pizarro, A. M.; Clarkson, G. J.; Sadler, P. J. *Organometallics* **2011**, *30*, 4702−4710.
(37) See the Supporting Information for details.
(38) Dadci, L.; Elias, H.; Frey, U.; Hörning, A.; Koelle, U.; Merbach, A. E.; Paulus, H.; Schneider, J. S. *Inorg. Chem.* **1995**, *34*, 306−315.
(39) Poth, T.; Paulus, H.; Elias, H.; Dücker-Benfer, C.; van Eldik, R. *Eur. J. Inorg. Chem.* **2001**, 1361−1369.
(40) Two diverging pK_a values were reported for $[IrCp^*Cl(bpy)]^+$: 6.86 (from NMR spectroscopy) and 7.5 (from UV−vis spectroscopy). See refs 34 and 35 for details.
(41) Masllorens, E.; Rodriguez, M.; Romero, I.; Roglans, A.; Parella, T.; Benet-Buchholz, J.; Poyatos, M.; Llobet, A. *J. Am. Chem. Soc.* **2006**, *128*, 5306−5307.
(42) Hull, J. F.; Himeda, Y.; Wang, W.; Hashiguchi, B.; Periana, R.; Szalda, D. J.; Muckerman, J. T.; Fujita, E. *Nat. Chem.* **2012**, *3*, 383−388.
(43) Keitz, B. K.; Bouffard, J.; Bertrand, G.; Grubbs, R. H. *J. Am. Chem. Soc.* **2011**, *133*, 8498−8501.
(44) Tulchinsky, Y.; Iron, M.; Botoshansky, M.; Gandelman, M. *Nat. Chem.* **2011**, *3*, 525−531.
(45) Tulchinsky, Y.; Kozuch, S.; Saha, P.; Botoshansky, M.; Shimon, L J. W.; Gandelman, M. *Chem. Sci.* **2014**, *5*, 1305−1311.
(46) Krüger, A.; Albrecht, M. *Aust. J. Chem.* **2011**, *64*, 1113−1117.
(47) As pointed out by one of the reviewers, the pH-dependent change in the amplitude of the DPV signals might suggest some behavior that is more complex than the expected pH effects. However, the Nernstian behavior of the complex points towards the latter.
(48) Bard, A. J.; Faulkner, L. R. *Electrochemical Methods: Fundamentals and Applications*; Wiley: Chichester, U.K., 2001.
(49) Huynh, M. H. V.; Meyer, T. J. *Chem. Rev.* **2007**, *107*, 5004−5064.
(50) Weinberg, D. R.; Gagliardi, C. J.; Hull, J. F.; Murphy, C. F.; Kent, C. A.; Westlake, B. C.; Paul, A.; Ess, D. H.; McCafferty, D. G.; Meyer, T. J. *Chem. Rev.* **2012**, *112*, 4016−4093.
(51) For an early example, see: Binstead, R. A.; Moyer, B. A.; Samuels, G. J.; Meyer, T. J. *J. Am. Chem. Soc.* **1981**, *103*, 2897−2899.
(52) Francas, L.; Sala, X.; Escudero-Adan, E.; Benet-Buchholz, J.; Escriche, L.; Llobet, A. *Inorg. Chem.* **2011**, *50*, 2771−2781.
(53) Diaz-Morales, O.; Hersbach, T. J. P.; Hetterscheid, D. G. H.; Reek, J. N. H.; Koper, M. T. M. *J. Am. Chem. Soc.* **2014**, *136*, 10432−10439.
(54) Joya, K. S.; Subbaiyan, N. K.; D'Souza, F.; de Groot, H. J. M. *Angew. Chem., Int. Ed.* **2012**, *51*, 9601−9605.
(55) Nakagawa, T.; Beasley, C. A.; Murray, R. W. *J. Phys. Chem. C* **2009**, *113*, 12958−12961.